

Journal of Climate Change, Vol. 9, No. 2 (2023), pp. 17-29. DOI 10.3233/JCC230012

Study of Palaeoclimate Reconstruction Using Sediments and Micropaleontology in the Karankadu Estuary, Ramanathapuram District, Tamil Nadu, India

Kongeswaran T.¹, Muthuramalingam R.^{1*}, Sivakumar K.¹, Venkatramanan S.², Muruganantham A.¹, Bangaru Priyanga S.¹ and Chandramohan S.²

¹Department of Geology, Faculty of Science, Alagappa University, Karaikudi, Tamil Nadu, India ²Department of Disaster Management, Alagappa University, Karaikudi, Tamil Nadu, India ⊠ muthurajendran147@gmail.com

Received February 10, 2023; revised and accepted March 28, 2023

Abstract: The study of sedimentary characteristics and paleontology is very useful in assessing the past environment of a study area. The Karankadu estuary study area is considered to be one of the most ecologically diverse in the Ramanathapuram district of southern India. The sedimentological and recent foraminiferal assemblages were studied using a drill core from the estuary. Foraminifera analyses, grain size analyses, heavy mineral analyses and XRD maps were prepared for the present study. A total of 30 species were identified from the following suborders: *Rotalina, Lagenina, Mollusca, Miliolina, and Textularina*. Grain size analysis identified the substrate as mostly silty clay. Heavy mineral analysis identified 90% of light minerals and 10% of heavy minerals. In XRD analysis, quartz and feldspar appeared as major minerals and garnet, zircon, hypersthene, magnetite and ilmenite as minor minerals. The present study shows that the environment is more diverse due to its quiet character and less responsive to hazardous events such as floods and waves.

Keywords: Paleo-environment; Biodiversity; Foraminifera; Heavy minerals; XRD.

Introduction

One of the fundamental views of geology is that the present is the key to the past. On documentation of the distribution of species in the present, we find that it is controlled by a combination of environmental variables. Understanding this, we can use this information to reconstruct past environments by using the fossilised representatives of modern organisms as paleoenvironmental indicators. This classical use of microfossils, along with biostratigraphy, is of great importance in the search for oil and gas. The microfossils contained in sediments can provide a great deal of information about past environments.

Microfossil assemblages are indicators of the physical and chemical conditions of their habitat and provide access to qualitative or quantitative reconstructions of environmental parameters. Calculations of the inventory and concentration of microfauna and microflora can incorporate the geochemical signature of the environment in which they originated. Biodiversity plays an important role in climate change adaptation and mitigation. In this study, biodiversity was investigated using foraminifera assemblages and sedimentological analyses. Foraminifera are unicellular protozoa that secrete a calcareous shell and were the most commonly recorded group. They are very diverse and are found in all oceans, from the coldest to the warmest. On

the other hand, clayey minerals from XRD analysis also have an impact on climatic changes. In recent few decades, benthic foraminifera assemblages have been used extensively to reconstruct current and past environmental conditions based on their composition, species diversity, and abundance, using a range of indices, statistical tests, and transfer functions (Buzas, 1969; Gibson and Buzas, 1973; Austin and Kroon, 1996; Weinkauf and Milker, 2018). The literature is peppered with records discussing the influence of size fraction on the benthic foraminifer assemblage and the extent to which this may affect environmental reconstructions (Jennings and Helgadottir, 1994; Knudsen and Austin, 1996; Bouchet et al., 2012). The coast is a unique environment where land, sea, and atmosphere constantly interact to influence a strip of space defined as a coastal zone. These coastal zones are important because they are the most dynamic and vulnerable to change from shifting terrestrial and marine processes, including human activities. Hurricanes, typhoons, tornadoes, storms, and tsunamis are the natural hazards that usually disrupt the coastal environment and ecosystem. On the other hand, the Fourth Assessment Report of the Intergovernmental Panel on Climate Change (IPCC) concluded that global climate changes have been observed in recent decades and thus can be projected into the future (IPCC, 2007). These changes, particularly temperature increases, are known to affect precipitation

variability (Allen and Ingram, 2002; Trenberth et al., 2003: Barnett et al., 2005), surface runoff (Nijssen et al., 2001), glacial and fluvial processes, soil erosion, and sediment load. An estuary is the marine-influenced portion of a drowned valley (Dalrymple et al., 1992). The estuary provides a rich biodiversity with various species of fish, crabs, shrimp, and different types of mangrove trees (Pramanik, 2019). Estuaries are now common at the mouths of rivers due to a relative rise in sea level since the last ice age. During this Holocene transgression, many river valleys were flooded and these provide a spectrum of morphologies and process controls that can be used to construct models of estuarine sedimentation. Two end members are recognised to be surge-dominated estuaries and tidaldominated estuaries. This study sought to investigate the distribution of microfossils, sedimentary feature type, mineralogical composition, depositional environment, and paleoclimate of the Karankadu estuary.

Study Area

The study area is the Karankadu estuary in the Thiruvadanai taluk of Ramanathapuram district, Tamil Nadu, India. The Karankadu tidal estuary is one of the most important tidal estuaries and also a center for picnic boats for tourism development. These tidal bays are connected to the mouth of the Pambar River. More

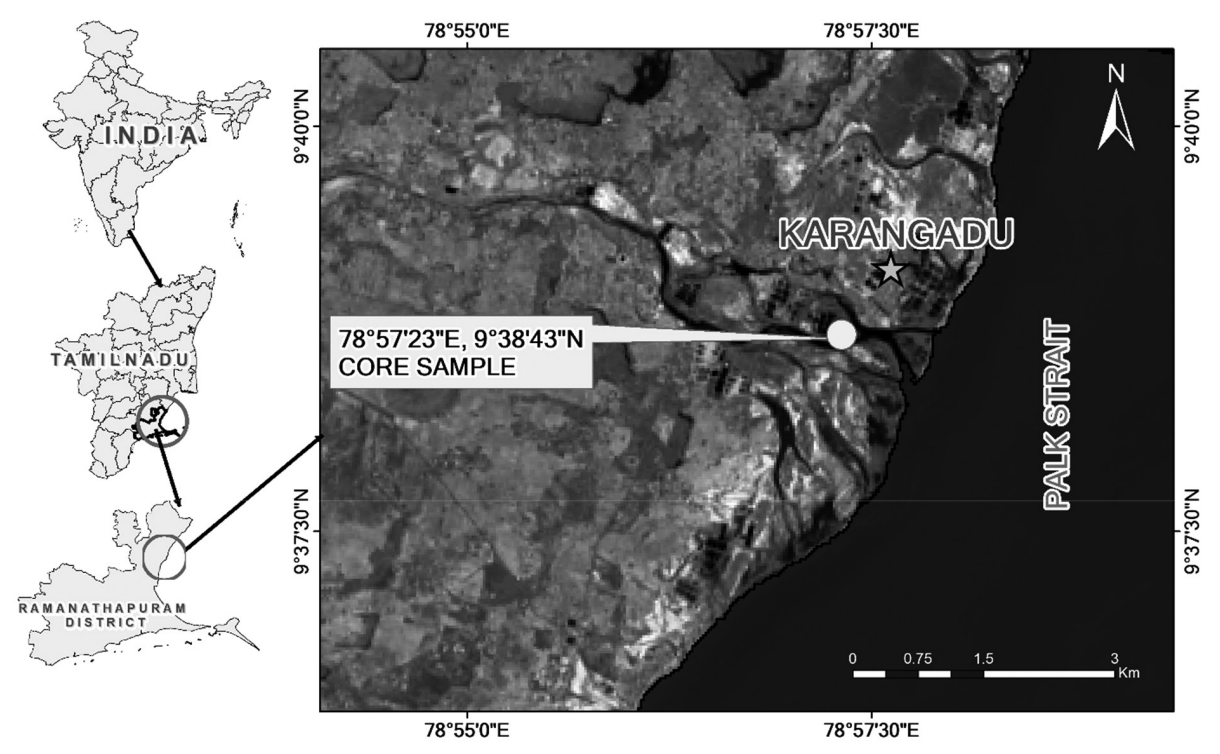


Figure 1: Core sample collected location map.

salt pans can be seen near the coastal village of Uppoor, which is adjacent to the study area. The tidal bays have been completely occupied by the mangrove forest. The mangrove forest represents a typical ecosystem in the coastal region. The study area has a tropical climate. In winter, there is much less rainfall in Ramanathapuram than in summer. In Ramanathapuram, the average annual temperature is 28.8°C. About 835 mm of precipitation falls annually. The geographical coordinates of the core sample are 78°57'23" E and 9°38'43" N.

Materials and Methods

Fieldwork was conducted in the Karankadu tidal bays to investigate geologic processes in the area and to collect sediment cores to determine texture, distribution of foraminiferal fauna, depositional environments, and paleoclimatology. During coring, the nature of tidal inlets and mangrove vegetation will also be monitored. Core samples were collected from the central portion of the tidal inlet using a boat that travelled to the site. Sediment cores were taken from the surface to a depth of 120 cm in a core tube (PVC - polyvinyl chloride). The core was manually pushed to depth to recover the samples. The core sample was further divided into 11 subsamples. When the core sample was collected, the speciation of the mangrove was also determined. The tidal tributary mangrove was fringed by numerous salt ponds and shrimp culture ponds. The collected sediment cores were subjected to texture analysis. Three types of sieves of mesh size 230, 400 and pan for sand, silt and clay sediments, respectively. At the same time, to separate the foraminiferal microfossils, the wet sediments are first treated with H₂O₂ to remove organic matter. Then heavy liquids CCl₄ (sp 2.4) are added to the sediments to float the foraminifera species from the sediments, and the separated foraminifera species were identified. Species identification and taxonomy were studied with reference to the present study (Lablich and Tappen, 1988) and other foraminifera literature. Based on fossil availability, sediment characteristics, and hydrodynamics of the coastal bay, the depositional environment was examined. The mineralogy of the sediments was investigated using the X-ray diffraction (XRD) method. The pulverised sediment cores were subjected to XRD examination, keeping the 2θ values between 0° and 80°. The d-spacing values and intensities were tabulated. The XRD method was also used to identify clay minerals, keeping the 2θ values from 0° to 30°. Furthermore, the core sediments were

analysed using bromoform heavy fluids (sp 2.89) to study the separation of heavy minerals.

Results and Discussion

The textures of the core sediments are sandy silt, silty clay, and clayey silt. Sandy silty substrate predominates in the core sediments from the surface to a depth of 0-37.5 cm. However, the bottom sediments from 87.5 cm to 120 cm core depth have a clayey silty substrate. Between 37.5 cm and 87.5 cm, the texture of the substrate is silty-loamy. The texture of the sediments of the core is shown in Table 1. The texture of the substrate is also shown in Figure 2 of the drill core. The texture of the substrate illustrates that the sediments at the top are fed by ocean currents and tides. The silt and clay content of the bottom can be controlled by the flow of the tidal inlet during the flood season. The Karankadu tidal inlets are one of the most important tidal inlets in the coastal wetland of Ramanathapuram district. The tidal bays are influenced by the ebb and flow of the tide or by the coastal currents and also by the rise and fall of the sea level at the new moon and full moon. Sometimes the tidal bays are also affected by storm surges, tsunamis, and also by marine transgression and regression. During these effects, depositional and erosional activities occur. During the diurnal and monthly effects of tides and currents, seawater may be trapped by the spit. At the same time, water from the adjacent salt pan is discharged into the tidal inlet. The saltwater becomes fresh water as the salinity is removed. This additional

Table 1: Texture of sediment core at various depths from 0 to 120 cm

S. No	Depth in (cm)	Sand (%)	Silt (%)	Clay (%)	Nature of substrate
1	2.5 cm	68	19	13	Sandy silt
2	12.5 cm	61	27	12	Sandy silt
3	25 cm	49	34	17	Sandy silt
4	37.5 cm	47	41	12	Sandy silt
5	50 cm	13	59	28	Silty clay
6	62.5 cm	12	51	37	Silty clay
7	75 cm	10	58	32	Silty clay
8	87.5 cm	11	51	38	Silty clay
9	100 cm	13	37	50	Clayey silt
10	112.5 cm	9	28	63	Clayey silt
11	120 cm	12	20	68	Clayey silt

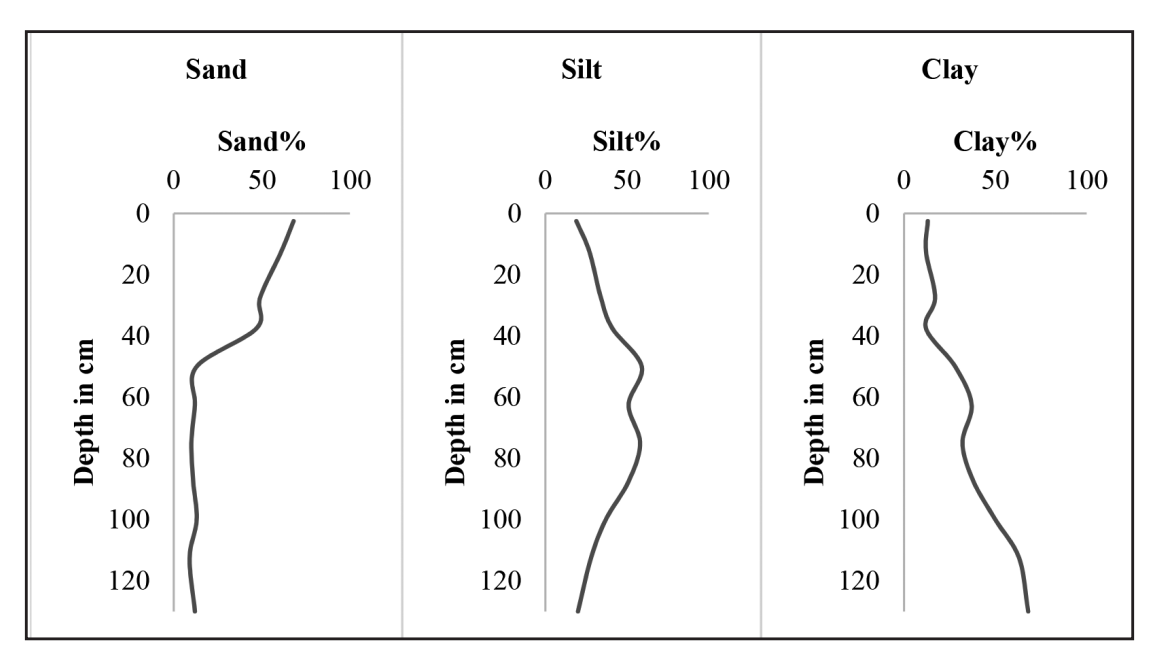


Figure 2: Downcore variation diagram of sand, silt and clay (%).

water in the tidal inlets causes the salinity of the water in the tidal inlets to become brackish water (salinity 15 to 29 parts per 1000 ml). Due to the brackish water environment, the mangrove plants *Salicornia* sp and *Vicennia* sp were grown. These plants are characterised by their pencil roots, also known as uprooted aerial roots. The seawater in the front part of the tidal inlet provides for the development of marine algae.

Micro-paleontological Analysis

Microfossils are a common feature of the geologic record from the Precambrian to the Holocene. They are most commonly found in marine deposits but also occur in brackish water, freshwater, and terrestrial sedimentary deposits. The study of foraminifera is the best way to study sedimentary deposits in the paleoenvironment. The general distribution of foraminifera is characteristic of an assemblage under marine influence and the dominance of Ammonia tepida indicates a tropical environment. Benthic foraminifera and gastropods are also used as tools to track transgression and regression events in lagoons connected to the open sea. The distribution of calcareous species indicates shallow environments with high water energy on hard substrates, especially on exposed, shallow roll forms. The following shallow marine species are widespread in post-tsunami sediments: Spiroloculina cummunis, Quinqueloculina lamarckiana, Ammonia beccarii, Ammonia tepida, Elphidium crispum. Bolivina, a species of the inner shelf, is a good indicator of strong marine environmental influence. Bolivina brittanica prefers muddy substrata and is restricted to bathyal and

marginal conditions. Most species have been fractured, indicating high-energy deposits that indicate the origin of the tsunami (Dawson, 1996). This tsunami-genetic sediment deposited on this coastal landform originated from the continental and inner shelf environments created by the tsunami. In the present study, the core sample was divided into 6 samples with equal intervals. The sample was coded as A (0-20 cm), B (20-40 cm), C (40-60 cm), D (60-80 cm), E (80-100 cm) and F (100-120 cm). A total of 11 families belonging to 30 benthic foraminifera and gastropod species were identified. Of the species collected, 57% were hyaline, 33% were porcelain, and 10% were calcareous. The largest population was found in the core samples of the estuary. The variation in the populations of all samples in the study areas is presented. The significant variation in the distribution of total and living species may be due to sedimentation as well as wave action and tidal flow. The genus Quinqueloculina, Triloculina and Spiroloculina is dominating the total assemblages followed by Ammonia, Asterorotalia, elphidium in the study region. Among these 30 species, Textularia agglutinants, Ouinqueloculina agglutinants, Arenaceous agglutinated species, Spiroculina communis, Spiroculina rotunda, Spiroculina indica, Quinqueloculina lamarckiana, Quinqueloculina seminulum, Quinqueloculina Costata, Ouinqueloculina sp, Triloculina trigonula, Triloculina tricarinata, Triloculina sp, Peneroplis planatus are calcareous, porcelaneous species and Ammonia beccari, Ammonia tepida, Ammonia dendata, Elpdium brispum, Elphidium advenum, Elphidium hispidula, Loxostomides, Lagena elongata, Lagena sp, Lagena bicarinata, Asterorotalia, Amphistegina mammilla, Amphistegina lessonii, Bolivina brittanica, Limacina trochiform are calcareous perforate species. List of the collected species are as follows (Tables 2 and 3):

Biodiversity Analyses

Paleontological statistics were used in this study to discuss species diversity. The Shannon-Wiener index H(S) is a measure of heterogeneity that considers the number of species and the distribution of individuals among those species (Murray, 1991).

Shannon Index (H) =
$$-\sum_{i=1}^{s} Pi \ln Pi$$

In the Shannon index, P is the proportion (n/N) of individuals found of a given species (n) divided by the total number of individuals found (N), In is the natural logarithm, Σ is the sum of the calculations, and s is the number of species. The diversity of the total 6 samples was examined using the statistical formula, and the result was discussed as a sample with a greater value, i.e., with greater diversity. According to the results of micropaleontological statistical analysis, the top sample of the drill core has a greater diversity than the other samples (Tables 4 to 8).

Table 2: Taxonomy chart of the collected species

Sub order	Super family	Family	Sub family	Genus	Species
Rotaliina	Rotaliacea	Rotalidae	Rotalinae	Ammonia	Ammonia beccarii
					Ammonia T
					Ammonia tepida
				Asterorotalia	Asterorotalia trispinosa
					Asterorotalia dendata
		Elphididae	Elphidinae	Elphidium	Elphidium crispum
					Elphidium advenum
					Elphidium hispidula
	Asterigerinoidea	Amphisteginidae	Amphistegininae	Amphistegina	Amphistegina mammilla
					Amphistegina lessonii
	Bolivinacea	Bolivinidae	Bolivininae	Bolivina	Bolivina brittanica
	Loxostomatacea	Loxostomatidea	Loxostomatinea	Loxostomum	Loxostomides
Lagenina		Lagenidae	Lageninae	Lagena	Lagena sp.
					Lagena elongata
					Lagena Bicarinata
Mollusca	Gastropods	Limacinidae	Limacininae	Limacina	Limacina reteroversa
					Limacina trochiform
Miliolina	Alveolinacea	Peneroplidae	Peneroplinae	Peneroplis	Peneroplis planatus
	Miliolacea	Spirolocolinidae	Spiroculininae	Spiroculina	Spiroculina communis
					Spiroculina rotunda
					Spiroculina indica
	Miliolacea	Hauerinidae	Quinqueloculininae	Quinqueloculina	Quinqueloculina Agglutinants
					Quinqueloculina lamarckiana
					Quinqueloculina costata
					Quinqueloculina seminulum
			Miliolinellinae	Triloculina	Triloculina trigonula
					Triloculina tricarinata
					Triloculina sp.
Textulariina	Textulariacea	Textulariidae	Textulariinae	Textularia	Textularia agglutinants
					Textularia sp.

Table 3: Number of the species in the core samples

S.No	Name of the species	Sample No-1	Sample No-2	Sample No-3	Sample No-4	Sample No-5	Sample No-6	Total number of species
1	Ammonia beccarii	3	4	6	8	9	11	41
2	Ammonia tepida	2	1	2	2	-	1	8
3	Ammonia dendata	1	-	2	-	2	2	7
4	Amphistegina mammilla	1	3	3	-	2	-	9
5	Amphistegina lessonii	-	1	1	4	-	3	9
6	Asterorotalia trispinosa	-	-	1	3	3	1	8
7	Asterorotalia dendata	1	3	2	2	4	-	12
8	Bolivina brittanica	2	1	-	4	5	3	15
9	Elphidium crispum	3	2	4	2	4	5	20
10	Elphidium hispidulum	1	-	2	-	1	-	4
11	Elphidium advenum	3	-	1	1	-	-	5
12	Lagena elongata	4	3	4	1	-	1	13
13	Lagena sp.	2	1	2		1	2	8
14	Lagena biccarinata	-	1	2	-	3	1	7
15	Limacina reteroversa	-	-	1	1	1	-	3
16	Limacina trochiform	3	2	-	1	3	2	11
17	Loxostomides	2	-	-	2	1	1	6
18	Qninqueloculina lamarckiana	4	1	4	3	7	7	26
19	Quinqueloculina agglutinants	2	2	4	1	3	4	16
20	Quinqueloculina	-	1	1	2	2	1	7
	costata							
21	Quinqueloculina seminulum	4	3	4	2	-	-	13
22	Peneroplis planatus	1	1	2	-	1	-	5
23	Spiroculina communis	3	3	5	6	5	7	29
24	Spiroculina rotunda	2	2	3	4	4	2	17
25	Spiroculina indica	-	1	1	2	1	1	6
26	Triloculina arigonula	3	4	7	5	7	6	32
27	Triloculina Tricarinata	-	1	-	3	2	4	10
28	Triloculina sp.	-	-	3	1	1	-	5
29	Textularia agglutinants	4	3	4	2	6	5	24
30	Textularia sp.	1	-	1	-	2	1	5
	Total species	52	44	72	62	80	71	381

Heavy Mineral and XRD Analysis

The heavy and light minerals analyzed by bromoform separation are quartz, and feldspar as light minerals and magnetite, ilmenite, garnet, zircon, hornblende and hypersthene as heavy minerals. The light mineral occurs in 90% while the heavy mineral occurs in 10% (Tables 9 to 15). The presence of light and heavy minerals in the study area indicates that the sediments were formed

Table 4: Shannon-Weiner Index calculation for sample - 1

	Sample No: 1									
S.No	Name of the genus	Number of individuals(n)	n/N (Pi)	Pi^2	ln Pi	Pi ln Pi				
1	Ammonia	6	0.115	0.013	-4.34	-0.499				
2	Amphistegina	1	0.019	0.0004	-7.82	-0.149				
3	Asterorotalia	1	0.019	0.0004	-7.82	-0.149				
4	Bolivina	2	0.038	0.001	-6.91	-0.263				
5	Elphidium	7	0.135	0.018	-4.02	-0.543				
6	Lagena	6	0.115	0.013	-4.34	-0.499				
7	Limacina	3	0.058	0.003	-5.81	-0.337				
8	Loxostomum	2	0.038	0.001	-6.91	-0.263				
9	Peneroplis	1	0.019	0.0004	-7.82	-0.149				
10	Quniqueloculina	10	0.192	0.04	-3.22	-0.618				
11	Spiroculina	5	0.096	0.01	-4.61	-0.443				
12	Triloculina	3	0.058	0.003	-5.81	-0.337				
13	Textularia	5	0.096	0.01	-4.61	-0.443				
		Total(N)=52				Total = -4.692				

Sample - 1; $H = -\Sigma Pi \ln Pi$; H = -(-4.692) = 4.692

Table 5: Shannon-Weiner Index calculation for sample - 2

	Sample No: 2									
S.No	Name of the Genus	Number of individuals(n)	n/N (Pi)	Pi^2	ln Pi	Pi ln Pi				
1	Ammonia	5	0.114	0.013	-4.34	-0.495				
2	Amphistegina	4	0.091	0.008	-2.40	-0.218				
3	Asterorotalia	3	0.068	0.005	-2.69	-0.264				
4	Bolivina	1	0.023	0.001	-3.77	-0.087				
5	Elphidium	2	0.045	0.002	-3.10	-0.140				
6	Lagena	5	0.114	0.013	-4.34	-0.495				
7	Limacina	2	0.045	0.002	-3.10	-0.140				
8	Loxostomum	0	0	0	0	0				
9	Peneroplis	1	0.023	0.001	-3.77	-0.087				
10	Quniqueloculina	7	0.159	0.025	-1.84	-0.618				
11	Spiroculina	6	0.136	0.02	-2	-0.443				
12	Triloculina	5	0.114	0.013	-4.34	-0.495				
13	Textularia	3	0.068	0.005	-2.69	-0.264				
		Total $(N) = 44$				Total = -3.746				

Sample - 2; $H = -\Sigma Pi \ln Pi$; H = -(-3.746) = 3.746

Table 6: Shannon-Weiner Index calculation for sample - 3

	Sample No: 3									
S.No	Name of the Genus	Number of individuals(n)	n/N (Pi)	Pi^2	ln Pi	Pi ln Pi				
1	Ammonia	10	0.139	0.019	-1.97	-0.274				
2	Amphistegina	4	0.056	0.003	-2.88	-0.161				
3	Asterorotalia	3	0.042	0.002	-3.17	-0.133				
4	Bolivina	0	0	0	0	0				
5	Elphidium	7	0.097	0.009	-2.33	-0.230				
6	Lagena	8	0.111	0.012	-2.20	-0.244				
7	Limacina	1	0.014	0.0002	-4.27	-0.060				
8	Loxostomum	0	0	0	0	0				
9	Peneroplis	2	0.028	0.001	-3.58	-0.100				
10	Quniqueloculina	13	0.181	0.033	-1.71	-0.310				
11	Spiroculina	9	0.125	0.02	-2.08	-0.260				
12	Triloculina	10	0.139	0.019	-1.97	-0.274				
13	Textularia	5	0.069	0.005	-2.67	-0.184				
		Total(N)=72				Total = -2.230				

Sample - 3; $H= -\Sigma Pi \ln Pi$; H= -(-2.230) = 2.230

Table 7: Shannon-Weiner Index calculation for sample - 4

	Sample No: 4							
S.No	Name of the Genus	Number of individuals(n)	n/N (Pi)	Pi^2	ln Pi	Pi ln Pi		
1	Ammonia	10	0.161	0.026	-1.655	-0.266		
2	Amphistegina	4	0.065	0.004	-2.733	-0.178		
3	Asterorotalia	5	0.081	0.007	-2.513	-0.204		
4	Bolivina	4	0.065	0.004	-2.733	-0.178		
5	Elphidium	3	0.048	0.002	-3.040	-0.146		
6	Lagena	1	0.016	0.0003	-4.135	-0.066		
7	Limacina	2	0.032	0.001	-3.442	-0.110		
8	Loxostomum	2	0.032	0.001	-3.442	-0.110		
9	Peneroplis	0	0	0	0	0		
10	Quniqueloculina	8	0.129	0.017	-2.048	-0.264		
11	Spiroculina	12	0.194	0.038	-1.640	-0.318		
12	Triloculina	9	0.145	0.021	-1.931	-0.280		
13	Textularia	2	0.032	0.001	-3.442	-0.110		
		Total $(N) = 62$				Total = -2.230		

Sample - 4; $H = -\Sigma Pi \ln Pi$; H = -(-2.230) = 2.230

Table 8: Shannon-Weiner Index calculation for sample - 5

	Sample No: 5								
S.No	Name of the Genus	Number of individuals(n)	n/N (Pi)	Pi^2	ln Pi	Pi ln Pi			
1	Ammonia	11	0.138	0.019	-3.963	-0.547			
2	Amphistegina	2	0.025	0.001	-6.908	-0.173			
3	Asterorotalia	7	0.088	0.008	-4.830	-0.425			
4	Bolivina	5	0.063	0.004	-5.521	-0.348			
5	Elphidium	5	0.063	0.004	-5.521	-0.348			
6	Lagena	4	0.05	0.003	-5.810	-0.291			
7	Limacina	4	0.05	0.003	-5.810	-0.291			
8	Loxostomum	1	0.013	0.002	-6.215	-0.081			
9	Peneroplis	1	0.013	0.002	-6.215	-0.081			
10	Quniqueloculina	12	0.15	0.023	-3.772	-0.566			
11	Spiroculina	10	0.13	0.017	-4.075	-0.530			
12	Triloculina	10	0.13	0.017	-4.075	-0.530			
13	Textularia	8	0.1	0.01	-4.605	-0.461			
		Total(N)=80				Total = -4.67			

Sample - 5; $H= -\Sigma Pi \ln Pi$; H= -(-4.672) = 4.672

Table 9: Shannon-Weiner Index calculation for sample - 6

Sample No: 6								
S.No	Name of the Genus	Number of individuals(n)	n/N (Pi)	Pi ²	ln Pi	Pi ln Pi		
1	Ammonia	14	0.197	0.039	-1.625	-0.320		
2	Amphistegina	3	0.042	0.002	-3.170	-0.133		
3	Asterorotalia	1	0.014	0.0002	-4.269	-0.060		
4	Bolivina	3	0.042	0.002	-3.170	-0.133		
5	Elphidium	5	0.070	0.005	-2.660	-0.186		
6	Lagena	4	0.014	0.0002	-4.269	-0.060		
7	Limacina	2	0.056	0.003	-2.882	-0.161		
8	Loxostomum	1	0.028	0.001	-3.576	-0.100		
9	Peneroplis	0	0	0	0	0		
10	Quniqueloculina	12	0.169	0.029	-1.778	-0.300		
11	Spiroculina	10	0.141	0.020	-1.959	-0.280		
12	Triloculina	10	0.141	0.020	-1.959	-0.280		
13	Textularia	6	0.085	0.007	-2.465	-0.210		
		Total(N)=71				Total = -2.22		

Sample - 6; $H= -\Sigma Pi \ln Pi$; H= -(-2.223) = 2.223

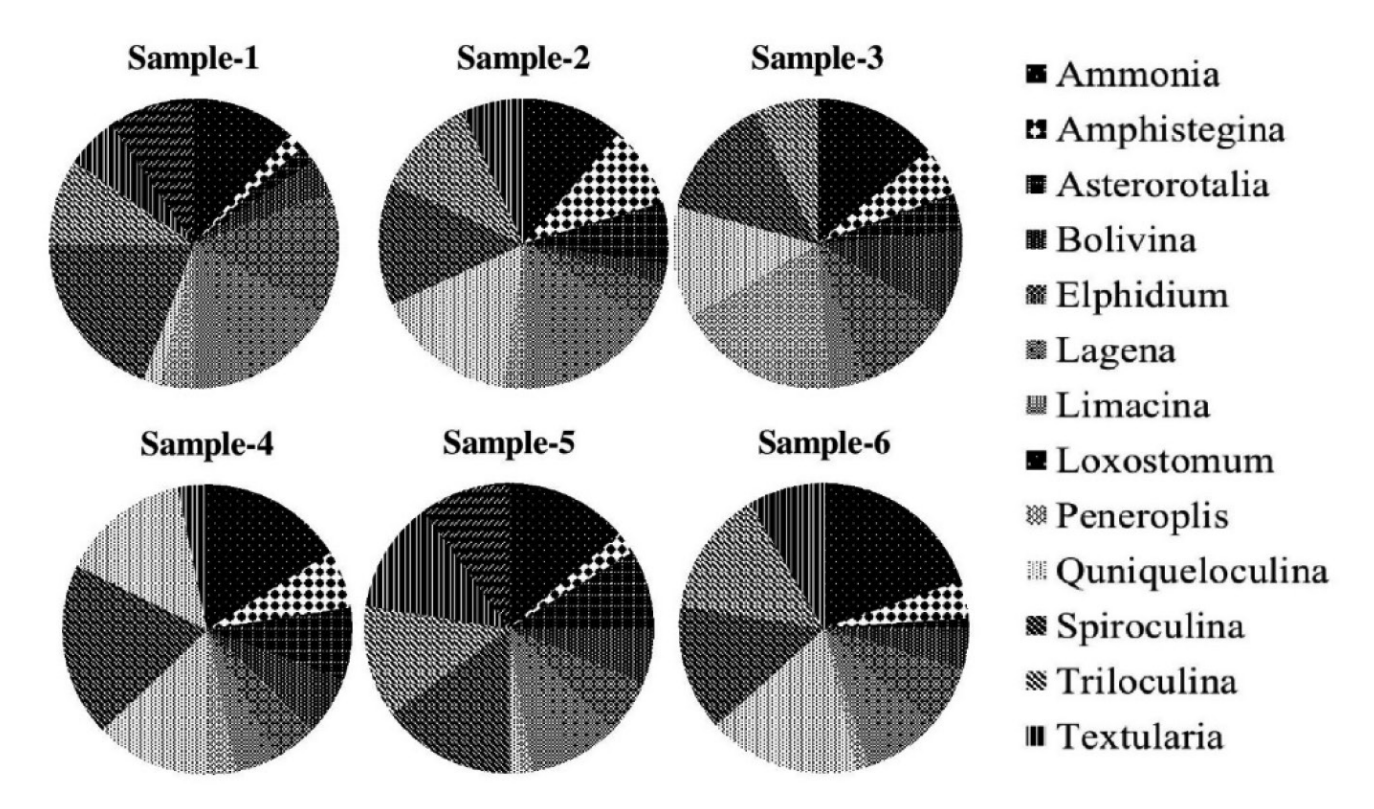


Figure 3: Pie diagram represents the genus assemblages in the samples.

from the source rock granite, charnockite, hornblendebiotite gneiss, quartzite and khondalite. The minerals are deposited by the river in the sea and redeposited by the waves and tides in the intertidal zones as placer minerals. The XRD results of the tidal inlet sediments can be found in the figures and the corresponding tables. The general XRD analysis shows a high proportion of quartz and feldspar and the remaining proportion of accessory minerals such as garnet, zircon, hypersthene, magnetite and ilmenite. Quartz has high erosion resistance; its presence indicates conditions with fast-flowing water (Al-Sudani and Albadran, 2014).

Sample: 1

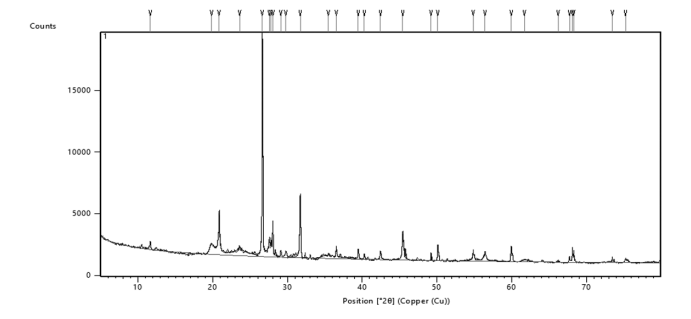


Figure 4: Graph showing the XRD result for sample -1.

XRD results of clay minerals indicate the presence of sepiolite, montmorillonite, and illite. The presence of illite and sepiolite indicates that they are derived from crystalline rocks containing feldspar and mica and from pre-existing soils and sedimentary rocks. The XRD of the clay minerals is shown in the figure. The clay mineral Precents indicates a warm tropical climate.

Table 10: Mineral identification for the XRD graph of sample - 1

Pos. [°2θ]	Height [cts]	d-spacing [Å]	Minerals
11.6297	589.55	7.60307	Bismutoferrite
20.8345	2358.96	4.26015	Sepiolite
26.6237	16417.62	3.34347	Quartz
27.7634	729.04	3.21068	Bismuth
28.0261	2373.85	3.18117	Sepiolite
31.6872	4407.37	2.82148	Cobaltite
39.4558	761.09	2.28201	Quartz
45.4136	1859.46	1.99551	Illite
50.1268	1283.35	1.81837	Quartz
59.9542	1227.26	1.54167	Biotite
68.1358	1172.66	1.3751	Clinoenstatite

Sample: 2

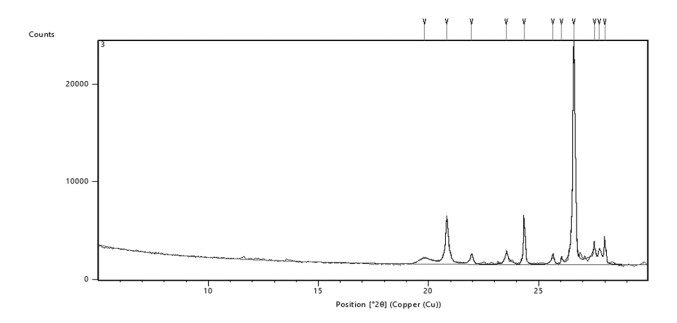


Figure 5: Graph showing the XRD result for sample -2.

Table 11: Mineral identification for the XRD graph of sample - 2

Pos. [°2θ]	Height [cts]	d-spacing [Å]	Minerals
20.8232	3694.58	4.26244	Chabazite
21.9493	808.39	4.04622	Illite
23.5323	878.58	3.77749	Calciborite
24.3352	4760.92	3.65466	oligoclase
25.6519	1457.1	3.46997	Brookite
26.0348	500.75	3.41979	Calciborite
26.5902	19926.24	3.34961	Quartz
27.5406	1397.11	3.23614	Bytownite
27.7563	1385.98	3.21148	Scapolite
28.0009	2517.91	3.18398	Chalcocite

Sample: 3

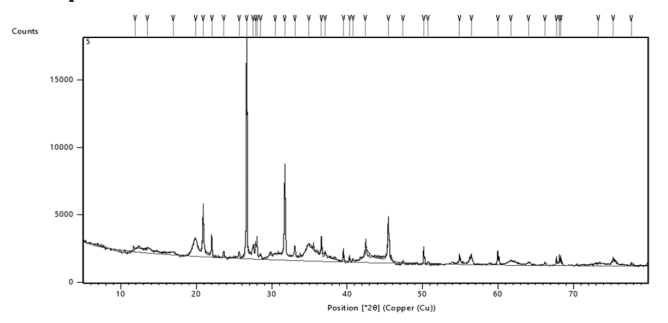


Figure 6: Graph showing the XRD result for sample -3.

Table 12: Mineral identification for the XRD graph of sample - 3

Pos. [°2θ]	Height [cts]	d-spacing [Å]	Minerals
20.8728	2476.82	4.25240	Orthoclase
22.0274	1503.16	4.03206	Labradorite
26.6547	15952.05	3.34165	Argentopyrite
28.0271	1255.21	3.18106	Sepiolite
31.7152	5901.81	2.81906	Borax

33.0580	904.49	2.70755	Andradite
36.5671	1192.75	2.45537	Quartz
42.3845	937.52	2.13085	Cuprite
45.4623	2885.42	1.99349	Halite
50.1567	1210.84	1.81736	Arsenopyrite
59.9694	1025.15	1.54131	Quartz

Sample: 4

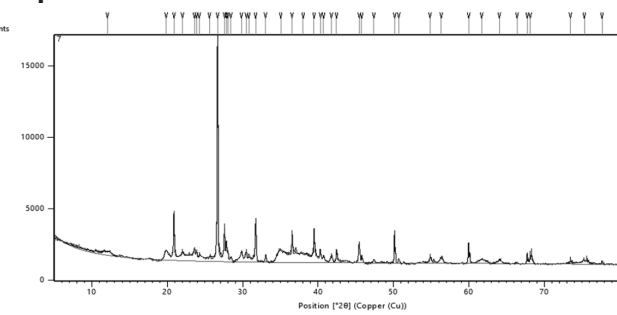


Figure 7: Graph showing the XRD result for sample -4.

Table 13: Mineral identification for the XRD graph of sample - 4

Pos. [°2θ]	Height [cts]	d-spacing [Å]	Minerals
20.8593	2547.02	4.25513	Orthoclase
24.2081	1029.07	3.67356	Glauconite
26.6428	13556.67	3.34312	Quartz
27.5803	1971.52	3.23157	Bytownite
27.8067	1042.02	3.20578	plagioclase
31.7051	2650.82	2.81993	Borax
39.4696	1028.96	2.28124	Quartz
40.3006	805.88	2.2361	Goethite
45.4422	1286.4	1.99432	Weissite
0.1435	2209.86	1.8178	Arsenopyrite
59.966	1483.77	1.54139	Quartz

Sample: 5

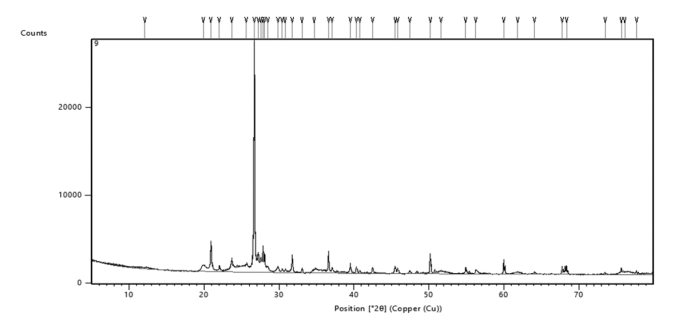


Figure 8: Graph showing the XRD result for sample -5.

(Contd.)

Table 14: Mineral identification for the XRD graph of sample - 5

Pos. [°2θ]	Height [cts]	d-spacing [Å]	Minerals
20.8913	2468.87	4.24869	Xonotlite
26.6892	22690.55	3.33742	Cassiterite
27.2283	2037.21	3.27255	Chalcopyrite
27.5743	1362.43	3.23226	Bytownite
27.8442	2507.77	3.20154	plagioclase
28.0612	1635.71	3.17728	Minuesotaite
31.74	1693.06	2.8169	Plumboferrite
36.6048	2277.12	2.45293	Lepidomelane
39.5098	1024.95	2.27901	Jamesonite
50.1779	2163.81	1.81664	Halite
59.9967	1649.37	1.54167	Quartz
67.7927	1030.05	1.38123	Pyrophyllite
68.3583	1575.93	1.37117	Lazurite

Sample: 6

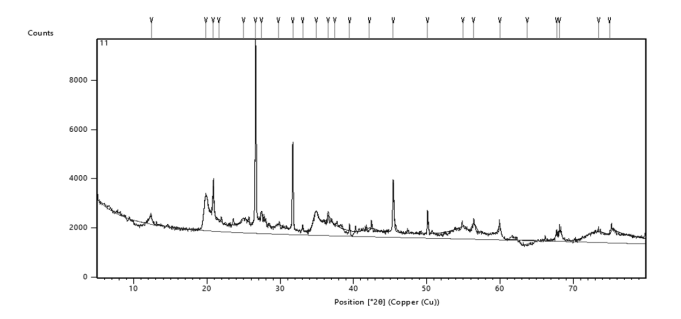


Figure 9: Graph showing the XRD result for sample -6.

Table 15: Mineral identification for the XRD graph of sample - 6

Pos. [°2θ]	Height [cts]	d-spacing [Å]	Minerals
19.8174	904.44	4.47644	Illite
20.8489	1302.46	4.25724	Orthoclase
26.6206	6120.11	3.34386	Quartz
31.6913	3155.27	2.82112	Malachite
45.4165	1853.28	1.99539	Illite
50.1285	970.84	1.81831	Quartz
54.9283	892.61	1.67023	Digenite
59.9907	678.72	1.54082	Quartz
68.105	1097.05	1.37565	Corundum
74.9787	9857.05	1.26566	Spessartine

Conclusion

The core sediments of the Karankadu tidal inlet show that sedimentation is controlled by both tidal currents and the river. Calcareous foraminifera predominates over siliceous foraminifera in the tidal inlet, indicating a warm tropical climate. The texture of the core shows a varied substrate of sandy silt, silty clay, and clayey silt. The clayey and silty substrate represents the sediments of land distribution during the flood period, while the sandy silt represents the tidal and coastal currents of the Palk Strait. The mineralogy of the sediments shows that the minerals are derived from the granite, charnockite and quartzite of the land resources. The XRD results also show that the minerals are derived from the sources of the alkaline rocks. The XRD results of the clay minerals show that the intertidal sediments are exposed to warm tropical climatic conditions. In general, extreme events such as storms or tsunamis can significantly alter hydrodynamic conditions and lead to rapid accumulation of sediments with significant changes in the accumulation of deep foraminifera and some gastropods. The Great Indonesian Earthquake triggered a tsunami wave across the Bay of Bengal on December 26, 2004, inundating the lowlands of the southeast coast of Tamilnadu. The recent Ockhi storm along the east coast of Kanyakumari may have also agitated the coast of the Gulf of Mannar, which may have led to the high-energy deposition throughout the study area, as indicated by the deposition of deep-sea fossils such as benthic foraminifera, some gastropods, and ostracods on the surface of the coastal regions along the southeast coast of Tamilnadu in December 2017. This group shows a similar association with environmental gradients. However, the benthic foraminifera shows a much stronger correlation. The benthic foraminifera is strongly correlated with changes in water depth, carbonate mud content, gravel content, organic carbon flux, temperature, and salinity. Application of a preservation index based on two foraminifera genera and accounting for both fragmentation and dissolution provide a good indication of the degree of sediment transformation. The consistency between species distribution and environmental variables, despite the high degree of degradation in many of the samples, provides much greater confidence in the application of benthic habitat mapping techniques to the Gulf of Mannar margin, where sedimentation rates are low and reworking is high. In the samples I have collected, the benthic foraminifera essentially exhibits Spiroculina communis, Quinqueloculina lamarckiana, Ammonia beccarii, Ammonia tepida, Elphidium crispum, Bolivina deep marine characteristics such as salinity, sublayer, temperature, depth, and habitat. Recently, these fossils occur in nearshore areas and beaches. High wave energy or an extreme event may be the trigger for the deposition of these deep-sea sediments in the sea or on the beach, leading to the conclusion that the sediments were deposited by a tsunami wave and storm and cyclone tides.

References

- Allen, M. and Ingram, W., 2002. Constraints on future changes in climate and the hydrologic cycle. *Nature*, **419**: 224-32. 10.1038/nature01092.
- Al-Sudani, K.J., Albadran, B.N., Jennifer, R. and Pournelle, J.R., 2014. Sedimentology and the sediments age study of Hareer's Tells, Southern Iraq. *Basrah Journal of Science*, **37(1):** 44-61.
- Anne, E.J. and Gudrun, H., 1994. Foraminiferal assemblages from the fjords and shelf of eastern Greenland. *Journal of Foraminiferal Research*, **24(2)**: 123-144. doi: https://doi.org/10.2113/gsjfr.24.2.123.
- Austin, W. and Kroon, D., 2001. Deep sea ventilation of the north-eastern Atlantic during the last 15,000 years. *Global and Planetary Change*, **-30**: 13-31. 10.1016/S0921-8181(01)00074-1.
- Barnett, T., Adam, J. and Lettenmaier, D., 2005. Potential impacts of a warming climate on water availability in snow-dominated regions. *Nature*, **438**: 303-309. 10.1038/nature04141
- Bouchet, V., Alve, E., Rygg, B. and Telford, R.J., 2012. Benthic foraminifera provide a promising tool for ecological quality assessment of marine waters. *Ecological Indicators*, **23:** 66-75. 10.1016/j.ecolind.2012.03.011.
- Dalrymple, R.W., Zaitlin, B.A. and Boyd, R., 1992. Estuarine

- facies models: Conceptual basis and stratigraphic implications. *J. Sediment. Petrol.*, **62:** 1130-1146.
- Gibson, T.G. and Buzas, M.A., 1973. Species diversity: Patterns in modern and miocene foraminifera of the Eastern Margin of North America. *Geological Society of America Bulletin*, **84:** 217-238.
- Knudsen, K.L. and Austin, W.E.N., 1996. Late glacial foraminifera. *In:* Andrews, J.T., et al. (eds.), Late Quaternary Palaeoceanography of the North Atlantic Margins. Geological Society Special Publication no. 111. London: The Geological Society, pp. 7-10.
- Loeblich, A.R. and Tappan, H., 1988. Foraminiferal genera and their classification. Springer, Berlin, 970 p. https://doi.org/10.1007/978-1-4899-5760-3.
- Martin A.B., 1969. Foraminiferal species densities and environmental variables in an estuary. *Limnology and Oceanography*, **14(3)**: 411-422.https://doi.org/10.4319/lo.1969.14.3.0411.
- Murray, J.W., 1991. Ecology and Palaeoecology of Benthic Foraminifera. Logman Scientific & Technical, London, 1-397.
- Nijssen, B., O'Donnell, G., Hamlet, A. and Lettenmaier, D., 2001. Hydrologic sensitivity of global rivers to climate change. *Climatic Change*, **50**: 143-175.10.1023/A: 1010616428763.
- Patrick, D., 1996. Beyond conventional change models: A processual perspective. *Asia Pacific Journal of Human Resources*, **34(2):** 57-70. https://doi.org/10.1177/103841119603400207.
- Pramanik, D.S., 2019. Fish species diversity and their assemblages of Devi estuary in north east coast of India. *International Journal Fisheries and Aquatic Studies*, 7: 265-273.
- Trenberth, K., Dai, A. Rasmussen, R. and Parsons, D., 2003. The Changing Character of Precipitation. Bull. Amer. Meteor. Soc. **84:** 1205-1217. 10.1175/BAMS-84-9-1205.
- Weinkauf, M.F.G. and Milker, Y., 2018. Benthic foraminifera assemblage in the >125 μm size fraction from the Pefka E section. PANGAEA, https://doi.org/10.1594/PANGAEA.884571.